

RSC Advances



This is an *Accepted Manuscript*, which has been through the Royal Society of Chemistry peer review process and has been accepted for publication.

Accepted Manuscripts are published online shortly after acceptance, before technical editing, formatting and proof reading. Using this free service, authors can make their results available to the community, in citable form, before we publish the edited article. This *Accepted Manuscript* will be replaced by the edited, formatted and paginated article as soon as this is available.

You can find more information about *Accepted Manuscripts* in the [Information for Authors](#).

Please note that technical editing may introduce minor changes to the text and/or graphics, which may alter content. The journal's standard [Terms & Conditions](#) and the [Ethical guidelines](#) still apply. In no event shall the Royal Society of Chemistry be held responsible for any errors or omissions in this *Accepted Manuscript* or any consequences arising from the use of any information it contains.

1 **Development of carbon adsorbents with high surface acidic and basic group**
2 **contents from phosphoric acid activation of xylitol**

3 Hai Liu^{a,b}, Jian Zhang^{*,a}, Li Jiang^a, Yan Kang^a, Cheng Cheng^a, Zizhang Guo^a, Chenglu Zhang^a

4

5 ^a*Shandong Key Laboratory of Water Pollution Control and Resource Reuse, School of*
6 *Environmental Science and Engineering, Shandong University, Jinan 250100, China*

7 ^b*Department of Chemical and Biomolecular Engineering, University of California, Berkeley,*
8 *California 94720, United States*

9 **Abstract**

10 The present paper evaluated the feasibility of synthesizing activated carbons from
11 xylitol with phosphoric acid activation at mild temperatures. Activation temperature
12 (250-450 °C) and phosphoric acid to xylitol impregnation ratio (0.2-3 wt.%) were
13 varied during the synthesis of xylitol-based activated carbon, and the effects of these
14 parameters on the textural and chemical properties of final activated carbons were
15 investigated by XRD, Raman, N₂ adsorption and desorption, SEM, XPS and Boehm's
16 titration. Results of yield, XRD and Raman indicated that phosphoric acid activation
17 enhanced the yields of activated carbons, and facilitated the formation of completely
18 carbonized materials at low temperatures (around 250 °C) by comparing with
19 charcoals derived from pyrolysis of xylitol. The porous structures of the activated
20 carbons were developed after activation, and for each activation temperature, the
21 carbons reached the maximum surface area at impregnation ratio of 1.5. Due to the

* **Corresponding author:** Tel.: +86 531 88363015; Fax: +86 531 88364513; E-mail address:
zhangjian00@sdu.edu.cn (J. Zhang); shandaliuhai@berkeley.edu (H. Liu)

1 strong oxidizing radicals decomposed from phosphates, the produced carbons contain
2 relatively high concentrations of acidic and basic surface groups. The total surface
3 groups peaked at 6.08 mmol/g for activated carbon obtained at activation temperature
4 of 350 °C and impregnation ratio of 1.5. The Ni(II) adsorption capacity of the
5 activated carbons were 4 to 7 folds of the charcoals.

6 **1. INTRODUCTION**

7 Activated carbon has been well proven to be one of the most effective adsorbents
8 toward a wide variety of organic and inorganic pollutants from aqueous or gaseous
9 environment due to its highly developed porous structure, low acid/base reactivity,
10 and wide spectrum of surface functional groups¹⁻³. In general, activated carbon
11 production consists of two processes: chemical activation and physical activation.
12 Due to the low reactivity between physical activating agents (H₂O or CO₂) and carbon
13 precursors, high activation temperatures (> 800 °C) and prolonged times are required
14⁴⁻⁶. Their high surface area comes at the cost of a high extent of char burn-off,
15 resulting in the low product yield and scarce surface functional groups. The chemical
16 activation usually takes place at lower temperatures (about 400-700 °C) in the
17 presence of an activating agent (ZnCl₂ or H₃PO₄). Therefore, the produced activated
18 carbons contain well-developed structure, high yield and favorable surface chemistry.
19 Given the environmental and economic effects, phosphoric acid activation has been
20 well demonstrated to be a promising method^{7,8}.

21 A various carbonaceous materials have been used as precursors to prepare
22 activated carbons by phosphoric acid activation, such as lignocellulosic materials^{9,10},

1 synthetic polymers^{11, 12}, and coals^{13, 14}. Impregnation and activation are the main
2 processes involved in phosphoric acid activation. During impregnation stage, H₃PO₄
3 permeates into the carbonaceous material and forms macromolecule composites. For
4 subsequent activation, H₃PO₄ reacts with precursor, resulting in favorable
5 physicochemical properties. Thus, the degree of impregnation affects dramatically the
6 activation effects^{15, 16}. Since these precursors are polymeric or extremely stable,
7 phosphoric acid is hard to react with them and penetrate into them at moderate
8 conditions. Zuo et al. has reported that the impregnation time of 10 h could result in
9 an 80% increase in surface area¹⁷. Therefore, in order to ensure good impregnation
10 effects, the impregnation is required 6-24 h. It has been also reported the activation
11 temperature should be controlled above 400 °C to ensure the produced activated
12 carbons with well-developed structure or good surface chemical properties¹⁸⁻²⁰. As a
13 result, producing activated carbon with phosphoric acid activation is a time and
14 energy-consuming process.

15 As the most important heterogeneous element, oxygen can form different
16 complexes with carbon, and result in acid-base and electron-donor/-acceptor
17 properties of activated carbon. Surface functional groups of activated carbon give
18 significant contribution to its adsorption ability, especially for low-size and positively
19 charged heavy metal ions^{21, 22}, primarily through providing adsorption sites of proton
20 exchange, electrostatic attraction, and surface complexation. Typical phosphoric acid
21 activated carbons exhibit a wide distribution of pore size, but relatively low metal ions
22 adsorption. Considering the huge influence of surface chemistry on the adsorption

1 performance of carbon materials, various modification methods have been developed
2 to increase surface oxygen content through pre- and post-treatment with gaseous or
3 liquid chemicals²³⁻²⁵. However, these methods require an additional process and are
4 also time and energy consuming process.

5 Organophosphorus compounds, as a kind of ester of phosphoric acid and alcohol,
6 have been well demonstrated to be novel activating agents for developing activated
7 carbons from lignocellulosic materials with relatively high surface oxygenated groups
8 and heavy metal ions adsorption capacities in comparison with reference activated
9 derived from H₃PO₄ activation in our previous works²⁶⁻²⁸. These favorable results
10 were mainly contributed to that radicals (R· and RO·) decomposed from phosphates
11 further created the porosity and surface functional groups of final carbons. In general,
12 the different properties of phosphoric acid-activated carbon mainly depend on the
13 precursor nature and synthesis conditions. Polyhydric alcohols contain multiple
14 hydroxyl groups, and they can condense with phosphoric acid via esterification to
15 form low molecular weight phosphates. These compounds can be easily decomposed
16 into phosphorus oxides and radicals. Based on these results, we deduce that these
17 reactions may promote the carbonization of polyhydric alcohols at low temperature,
18 and enhance the surface oxygen contents of the produced carbon materials, eventually
19 increasing their adsorption abilities toward heavy metal ions. In addition, polyhydric
20 alcohols can be melted at low temperatures (above 93 to 95 °C) and dissolves easily in
21 phosphoric acid solution (eg. 85 wt.%)²⁹. Thus, via phosphoric acid activation, using
22 polyhydric alcohols as carbon precursors may avoid the problem of long impregnation

1 time and high activation temperature for production of activated carbon from
2 conventional lignocellulosic materials. However, little information is available on
3 preparation of activated carbon from phosphoric acid activation of polyhydric
4 alcohols.

5 Accordingly, a common polyhydric alcohol, xylitol, was chosen as carbon
6 precursor. Xylitol (formula, $\text{CH}_2\text{OH}(\text{CHOH})_3\text{CH}_2\text{OH}$) is categorized as a polyalcohol
7 or sugar alcohol. The main goals of the present work are to evaluate the feasibility of
8 preparation of activated carbon from xylitol with phosphoric acid activation, and to
9 provide a full understanding of the chemical properties and structural characteristics
10 of the carbons. For these purposes, the thermal behaviors of xylitol treated with
11 different impregnation ratios of phosphoric acid were studied. The effects of
12 impregnation ratio and activation temperature on the development of pore structure
13 and chemical characteristics were also investigated. The synthesized carbon materials
14 were characterized by X-ray diffraction (XRD), N_2 adsorption and desorption,
15 scanning electron microscopy (SEM), X-ray photoelectron spectroscopy (XPS), and
16 analysis of Boehm's titration.

17 **2. EXPERIMENTAL (MATERIALS AND METHODS)**

18 **2.1. Synthesis of Carbon Adsorbents**

19 In a typical synthesis, activated carbons were prepared by phosphoric acid
20 activation of xylitol. Five grams of xylitol was mixed fully with phosphoric acid
21 solution (85 wt.%) at a impregnation ratio of 0.2:1 - 3:1 (g H_3PO_4 / g xylitol). The
22 nomenclature for the impregnated samples (xylitol-R) was the xylitol followed by a

1 number indicating the impregnation ratio. After mixing, xylitol-R samples were
2 immediately heated (heating rate of 10 °C/min) from room temperature to the desired
3 temperature and maintained at this temperature for 1 hour under nitrogen atmosphere
4 (100 mL/min) in a tube furnace. After cooling to room temperature, the samples were
5 washed with deionized water until steady pH and absence of phosphate anions.
6 Finally, the samples were dried at 105 °C for 9 h and grounded to obtain the particle
7 size of 100/160 mesh (Model Φ 200). The activated carbons obtained at activation
8 temperature of X °C with impregnation ratio of R were referred to as AC-X-R. In
9 order to evaluate the effect of phosphoric acid activation on the characteristics of final
10 carbon materials, the charcoals (C-X) were also prepared by pyrolysis of xylitol at the
11 same heating conditions.

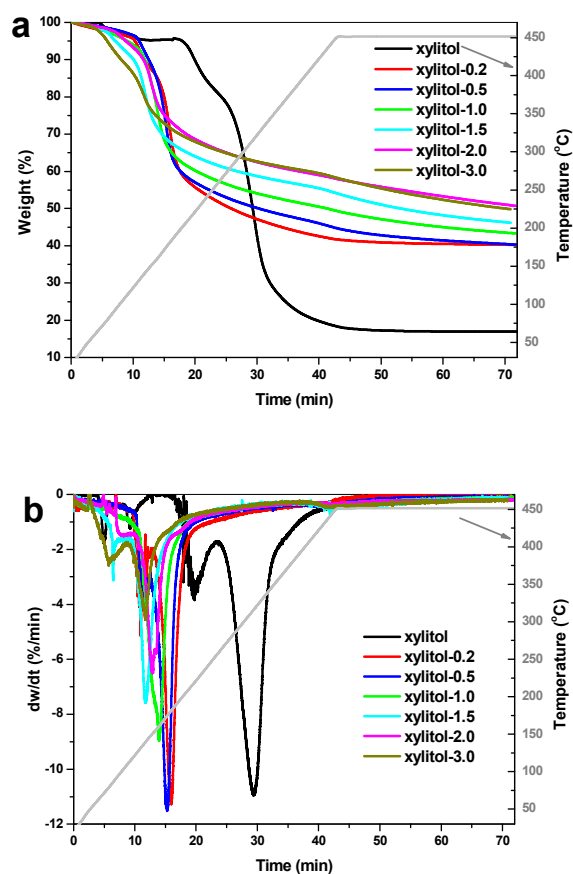
12 **2.2. Characterization**

13 The thermal behaviors of the untreated xylitol and xylitol-R samples during
14 carbonization/activation were evaluated with a thermal analyzer (TGA-50 analyzer).
15 Samples were heated at a heating rate of 10 °C/min under nitrogen atmosphere (100
16 mL/min). The crystallinity of the produced AC-X-R samples was investigated by
17 using a Rigaku D/MAX-YA diffractometer with Ni-filtered Cu K α radiation as X-ray
18 source. Raman spectra were collected with a Raman microscope (633 nm laser
19 excitation, Renishaw inVia Raman microscope, UK). The textural properties were
20 determined by N₂ adsorption/desorption at 77 K with a surface area analyzer
21 (Quantachrome Corporation, USA). The structure and morphology were examined by
22 a scanning electron microscopy (SEM) JSM-5610LV (10 kV, Jeol Company, Japan).

1 The oxygenated acidic and basic surface groups were determined using the Boehm's
2 titration method³⁰. The surface elemental composition was studied by using an X-ray
3 photoelectron spectrometer (XPS, Perkin-Elmer PHI 550 ESCA/SAM) with Mg Ka
4 irradiation source. All the spectra were calibrated by setting C 1s to 284.6 eV. The
5 adsorption abilities of the carbon adsorbents were evaluated by batch Ni(II)
6 adsorption experiment.

7 3. RESULTS AND DISCUSSION

8 3.1. Thermal Analysis



9

10

11 **Fig. 1. TGA (a) and DTG (b) curves for pyrolysis of xylitol and xylitol-R samples.**

12

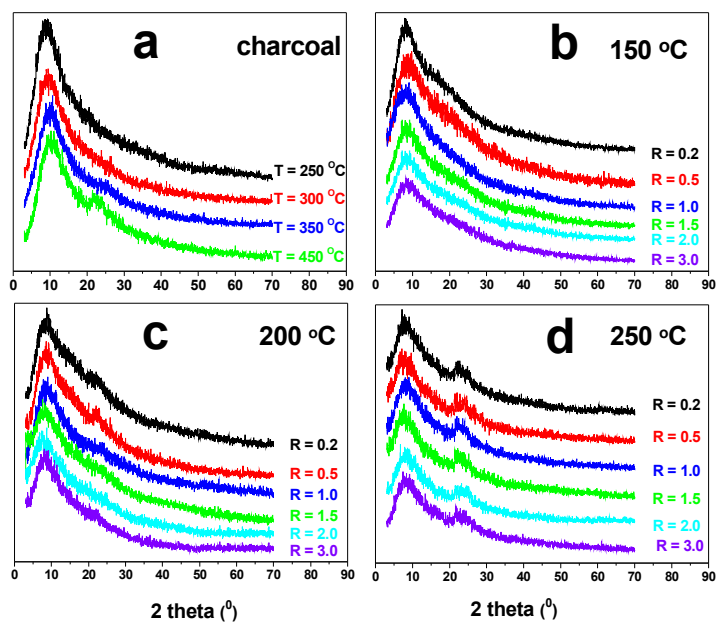
13 The thermogravimetric analysis (TGA) and derivative thermogravimetric (DTG)

1 curves of the original and H₃PO₄-impregnated xylitol samples are shown in Fig. 1. It
2 can be seen from Fig. 1a that the weight loss for original xylitol began at temperature
3 slightly higher than its boiling point of 216 °C, its weight loss rate slowed down as
4 temperature above 350 °C (Fig. 1b), and a slight weight was observed when
5 temperature was kept at 450 °C, indicating that the carbonization process was
6 completed. However, the xylitol-R samples showed a major weight loss at
7 temperature below 200 °C, which reflected that phosphoric acid promoted
8 carbonization at low temperatures. From room temperature to about 100 °C, an initial
9 weight loss was mainly due to the loss of moisture present in the xylitol-R samples.
10 Some reactions were expected to be responsible for the dramatic weight loss for
11 pyrolysis of xylitol-R samples at temperature below 250 °C: (1) esterification between
12 phosphoric acid and xylitol, which took place at temperatures above about 90 °C; (2)
13 etherification between hydroxyl groups of xylitol catalyzed by phosphoric acid; and
14 (3) condensation between phosphoric acid molecules (occurred at temperature above
15 213 °C). Meanwhile, the produced phosphates with low polymerization degree were
16 instable at high temperature, and subsequently volatilized and decomposed into
17 radicals and P₂O₅^{31, 32}, causing a further weight loss.

18 The thermal behaviors of xylitol-R samples were obviously different to other
19 phosphoric acid-impregnated lignocellulose/coal samples^{31, 33}. During activation,
20 xylitol formed easily phosphates with low polymerization degree, which tended to
21 volatilize and decompose and led to less phosphoric compounds remaining in the
22 samples. The loss of phosphorous species and production of radicals by

1 decomposition of phosphates resulted in: (1) carbonization of xylitol at low
 2 temperature (see Fig. 2) (2) low yield (see Fig. 3); (4) suppressed formation of porous
 3 structure (see Fig. 4); (3) low surface phosphorus content (see Fig. 6); and (4) large
 4 surface oxygen content (see Fig. 6) for final carbon materials.

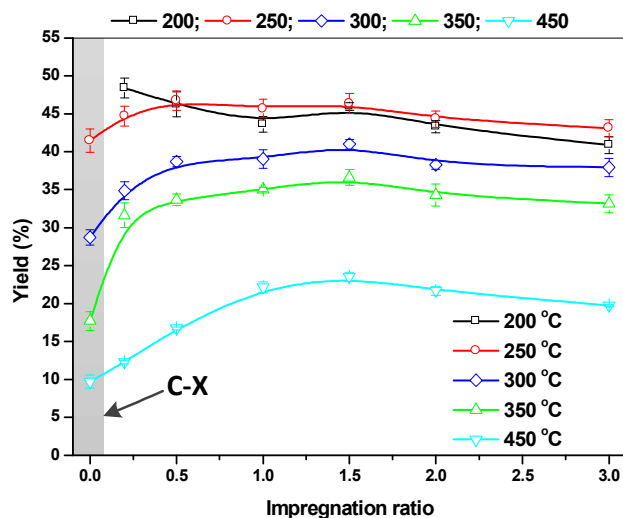
5 3.2. Formation of Carbon Materials



6
 7 **Fig. 2.** XRD patterns of charcoals (a) derived from pyrolysis of xylitol and AC-X-R samples
 8 produced at activation temperatures of 150 (b), 200 (c), and 250 °C (d).
 9

10 As shown in Fig. 2, a broad peak at around $2\theta = 23^\circ$ can be found from XRD
 11 patterns of some samples, which was attributed to (002) planes of the graphitic
 12 crystallites³⁴, and revealing that these xylitol or xylitol-R samples have been
 13 carbonized or activated into carbon materials. All samples exhibited an intense and
 14 sharp peak at around $2\theta = 10^\circ$, which was attributed to the water molecular or
 15 oxygen-containing groups between the layers of the graphite. It can be seen from Fig.

1 2a that for the C-X samples obtained at carbonization temperature below 350 °C, they
2 exhibited a XRD pattern without (002) diffraction peak, reflecting that the final
3 materials were carbonized incompletely. After phosphoric acid activation, absent,
4 inconspicuous and broad (002) diffraction peaks were recognized for the AC-150-R,
5 AC-200-R and AC-250-R samples (Fig. 2b, c and d), respectively. These results
6 meant that phosphoric acid activation promoted the carbonization of xylitol at low
7 temperatures, and the onset of complete carbonization of xylitol-R samples took place
8 between 200 and 250 °C. The AC-250-R samples also exhibited typical Raman
9 spectra of non-graphitic carbon materials (Shown in Supporting Information (SI)
10 Figure S1). This can be also confirmed by the yield analysis that the yields of
11 AC-200-R samples were slightly lower than that of AC-250-R samples (Fig. 3).
12 Obviously, high activation temperature will promote the weight loss of xylitol-R
13 samples (see Fig. 1). However, xylitol could not be incompletely carbonized at low
14 activation temperature, hence some dissolved organic matters were removed from the
15 solid products by DI water washing. Accordingly, it also can be deduced that
16 AC-200-R samples were incomplete carbonized products. It is well known that xylitol
17 has a very low melting point (93~95 °C) and can be dissolved in phosphoric acid
18 solution easily. Thus, xylitol can be mixed fully with phosphoric acid, which
19 promoted the reactions between xylitol and phosphoric acid. In addition, the formed
20 phosphates decomposed into strong oxidizing radicals, and further enhanced the
21 carbon structure forming at low temperature. Accordingly, the precursor exhibited
22 high weight loss and formed carbonized structures at low temperatures.



1

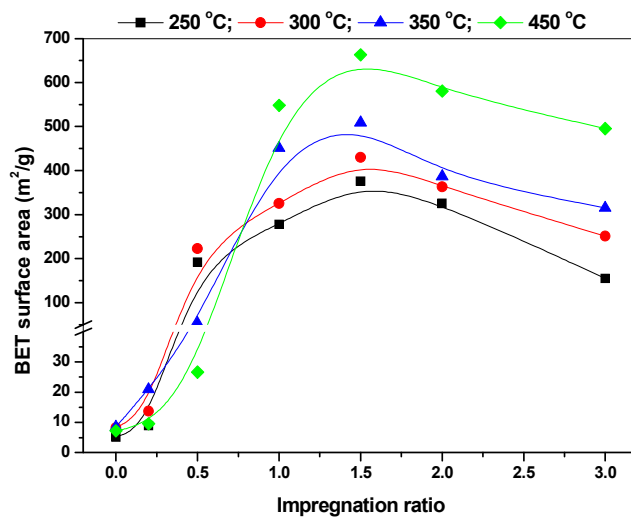
2 **Fig. 3. Yields of the produced carbon materials (Yield is defined as the % ratio of weight of**
 3 **carbon produced to the weight of xylitol utilized for activation/pyrolysis).**

4

5 The yields of the carbon materials are represented in Fig. 3. The yields of AC-X-R
 6 samples were obviously higher than that of C-X samples, especially at high activation
 7 or carbonization temperatures, meaning the good flame-retardant effect of phosphoric
 8 acid. This was due to that phosphoric acid promoted formation of carbon materials at
 9 low temperatures, hence increasing the yields of AC-X-R samples. For each
 10 activation temperature, with increasing impregnation ratio up to 3, the yield of the
 11 samples increased to a maximum at impregnation ratio of 1.5 and decreased slightly at
 12 higher impregnation ratios, because suitable dose of phosphoric acid had a positive
 13 effect on the yield, while the excessive dose resulted in the highly aggressive
 14 chemical reactions between the xylitol and phosphoric acid. For each impregnation
 15 ratio, the yield decreased dramatically as the reaction temperatures increased due to
 16 the enhanced decomposition of precursor at higher temperatures. It should be noted
 17 that AC-250-R, AC-300-R and AC-350-R samples had relatively high yields (30-45%)

1 due to the low activation temperatures. However, the samples produced at activation
2 temperature of 450 °C had low yields (10-20%). The yields of xylitol-based activated
3 carbons were much lower than the activated carbon derived from lignocellulose
4 materials (30-50%) at activation temperature of 450 °C, such jackfruit peel waste¹⁸,
5 Kraft lignin³⁵, date stones³⁶, and rubber wood sawdust³⁷. As proposed above, the
6 oxidizing radicals derived from decomposition of phosphate esters accelerated the
7 weight loss of xylitol-R samples, and the volatilization of organophosphorus esters
8 also caused the relatively low yields of final carbon materials. Taking into account the
9 yield and completely carbonized products, the activation temperature was
10 recommended in the range of 250 - 450 °C for phosphoric acid xylitol-based carbon
11 material production.

12 3.3. Physical Properties of Activated Carbons

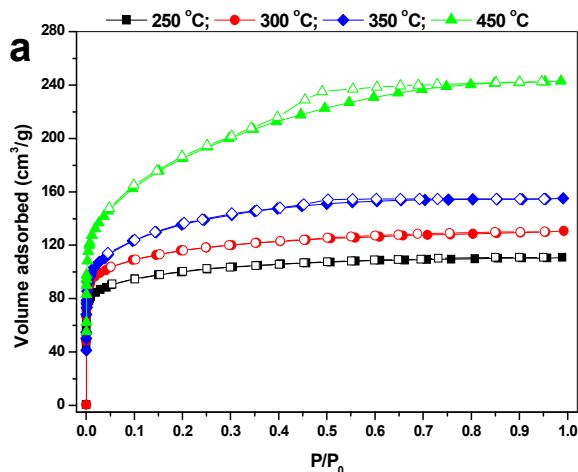


13
14 **Fig. 4. BET surface area calculated by the standard BET method of the carbon materials.**

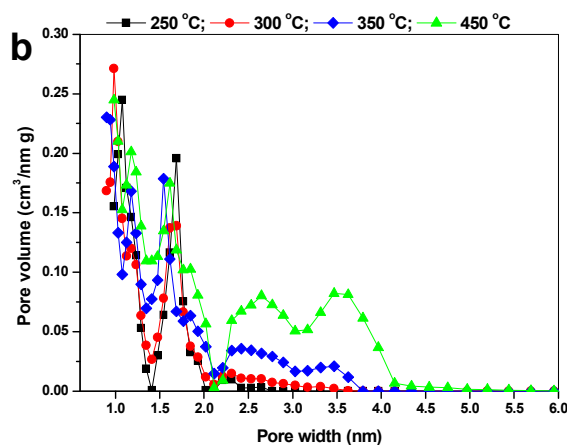
15
16 The effects of impregnation ratio and activation temperature on the BET surface
17 area (S_{BET}) of the samples are shown in Fig. 4. At each activation temperature, the

1 S_{BET} of carbons reached a maximum at an impregnation ratio of approximately 1.5,
2 which was coincident with the results of yield. The same tendency was observed
3 previously for activated carbons produced from phosphoric acid activation of cotton
4 stalks³², hydrochars³⁸, and cellulose³⁹. It can be seen that phosphoric acid activation
5 developed the porous structure of final carbon materials (AC-X-R) as compared to the
6 C-X samples (less than 10 m²/g), particularly for the AC-X-R samples with R beyond
7 a value of 0.5. Such results can be also observed from the SEM images for the C-X
8 and AC samples (shown in SI Figure S2). With impregnation ratio below 0.5, the
9 carbonization/activation was incomplete/ inadequate for original xylitol and
10 xylitol-X-0.2 samples, demonstrated by their low surface area (less than 30 m²/g).
11 Some phosphoric acid or phosphorous species in xylitol-R was lost via decomposition
12 and volatilization of phosphates. Thus, detectable activation in the terms of porous
13 structure was not obtained for xylitol-X-0.2 samples. Such phenomenon can be also
14 observed from the S_{BET} of AC-X-0.5 samples that the S_{BET} values of AC-250-0.5 and
15 AC-300-0.5 samples were much larger than AC-350-0.5 and AC-450-0.5 due to the
16 loss of phosphoric acid and the consequent damage of pore structure at high activation
17 temperatures. An increase in impregnation ratio enhanced degree of polymerization of
18 phosphates, and restrained their thermal decomposition, resulting in the higher yield
19 and surface area. However, the excessive phosphoric acid addition aggravated such
20 activation effect and destroyed some pores³². The surface area of carbons increased
21 with increasing activation temperature was mainly due to the enhanced interactions of
22 phosphoric and xylitol. This trend was generally consistent with previous reports for

1 phosphoric acid activation of Kraft lignin³⁵, chestnut wood⁴⁰, and rice straw^{41,42}.



2



3

4 **Fig. 5. N₂ adsorption/desorption isotherms (a) and DFT pore size distributions (b) for**
5 **carbons prepared with impregnation ratio of 1.5 at different activation temperatures.**

6

7 Nitrogen adsorption and desorption isotherms and DFT pore size distributions of
8 the carbons produced at different activation temperatures using an impregnation ratio
9 of 1.5 are summarized in Fig. 5. The isotherms for AC-250-1.5 and AC-300-1.5 were
10 Type I, practically without hysteresis loop, which was characteristic of highly
11 microporous carbons. The isotherms for AC-350-1.5 and AC-450-1.5 were the
12 mixture of Type I and IV, with a hysteresis at P/P₀ above 0.4 (Fig. 5a), indicating a

1 micro-mesoporous structure. These results also can be confirmed from Fig. 5b that the
 2 pore widths of a large part of pores for AC-350-1.5 and AC-450-1.5 were in the range
 3 of 2-6 nm, as will be demonstrated by the evaluated parameters (see Table 1). The
 4 structural characterization results listed in Table 1 showed that with the increase of
 5 temperature from 250 to 450 °C, the micropores and mesopores of the carbons were
 6 developed, but the contribution of micropore to the total porosity (V_{mic}/V_{mes})
 7 decreased, suggesting the enlargement of existing micropores as well as the
 8 continuous pore creation.

9

10 **Table 1-Textural parameters of activated carbons prepared with impregnation ratio of 1.5 at**
 11 **different activation temperatures.**

Carbon	S_{BET} (m ² /g)	S_{mic} (m ² /g)	%	S_{ext} (m ² /g)	%	V_{tot} (cm ³ /g)	V_{mic} (m ³ /g)	%	V_{ext} (m ³ /g)	%
AC-250-1.5	377	372	98.7	5	1.3	0.171	0.165	96.5	0.006	3.5
AC-300-1.5	432	380	88.0	52	12.0	0.202	0.169	83.7	0.033	16.3
AC-350-1.5	509	403	79.2	106	20.8	0.248	0.173	69.8	0.075	30.2
AC-450-1.5	663	433	65.3	230	34.7	0.376	0.178	47.3	0.198	52.7

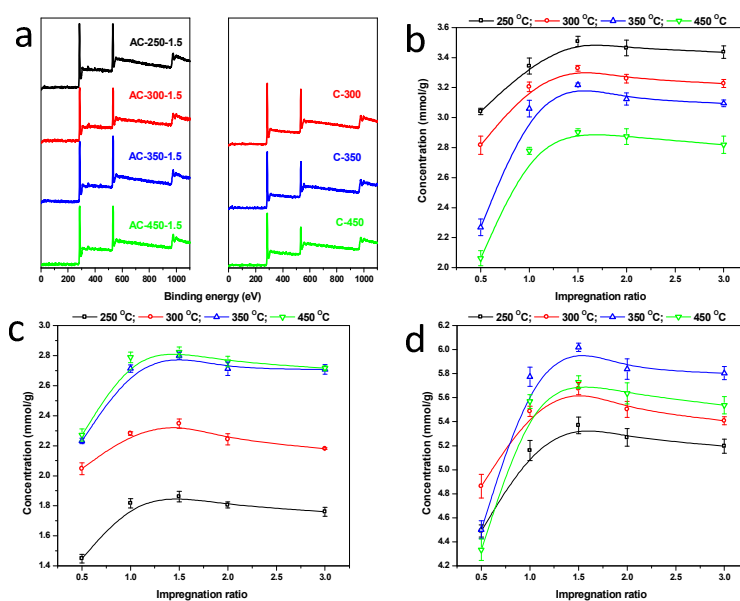
The micropore surface area (S_{mic}), external surface area (S_{ext}) and micropore volume (V_{mic}) were evaluated by the t-plot method. Total pore volume calculated for $P/P_0 = 0.95$. Mesopore volume (V_{mes}) was calculated by $V_{tot} - V_{mic}$.

12

13 The simultaneous increases of micropore and mesopore volumes were related to
 14 the geometry of polymeric species (polyphosphoric acids) and the production of
 15 volatile substances. By condensation and dehydration, phosphoric acid (H₃PO₄)
 16 converted to polycondensed forms: pyrophosphoric acid (H₄P₂O₇) and polyphosphoric
 17 acid (H_{n+2}P_nO_{3n+1}) at temperature above 213 °C, and metaphosphoric acid ((HPO₃)_n) (>
 18 300 °C)³¹. After thermal treatment, the acids occupied different volumes in the
 19 carbonized materials were extracted by washing, and produced different porosities.

1 The higher activation temperature promoted the condensation and dehydration of
 2 phosphoric acid, hence causing the formation of larger pores. Thus, evident pore
 3 evolution occurred as activation temperature was above 300 °C. Meanwhile,
 4 phosphoric acid formed cross-linked structure with polyhydric alcohol (xylitol), and
 5 the enhanced elimination of highly volatile matters at higher activation temperatures
 6 further promoted the porosity of final carbons.

7 3.4. Chemical Characteristics



8
 9 **Fig. 6.** XPS survey spectra of C-X and AC-X-1.5 samples (a). The Boehm's titration results
 10 of the carbons: acidity (b), basicity (c), and total groups (d).
 11

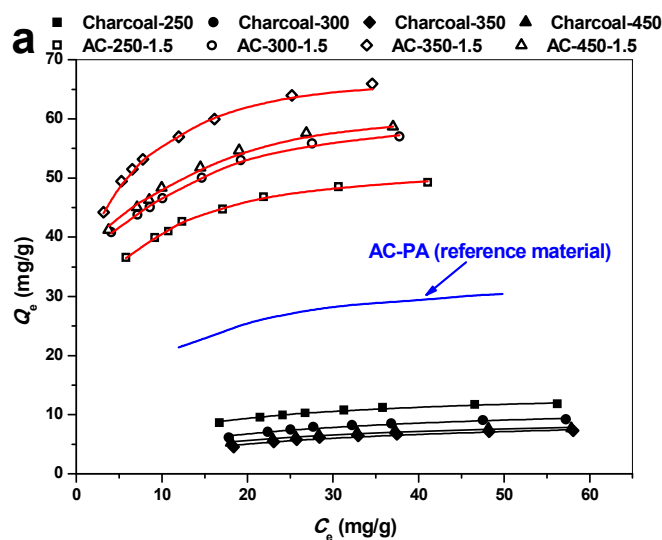
12 The surface compositions of the carbons were also determined by XPS shown in
 13 Fig. 6. The spectra indicated the presence of two distinct peaks for carbon and oxygen
 14 elements, and the contribution of other elements was insignificant, meaning the
 15 functionalities were derived from the complexes of carbon and/or oxygen. Obviously,
 16 in comparison with C-X samples, the much higher intensity of O 1s peaks for the

1 activated carbons derived from same heating conditions indicated that they contained
2 more oxygen containing groups. The XPS can only reflect the oxygen functionalities
3 on the outer surface of the samples. The activated carbons exhibited porous structure
4 and the C-X samples were almost nonporous. It meant the activated carbons exhibited
5 extra more total oxygen groups than C-X samples. For the phosphoric acid activated
6 carbons, high phosphorus content (1-8 wt.%) were detected on their surfaces^{7, 43, 44}.
7 However, the activated carbon studied in present paper was absent of phosphorus
8 species, which can be attributed the formation, and subsequent volatilization and
9 decomposition of phosphate esters.

10 In order to evaluate quantitatively the surface functionalities of the carbon
11 influenced by the preparation parameters, both acidic and basic groups of the
12 activated carbon were determined by Boehm' titration. It is known that the acidity of
13 activated carbon mainly derive from the carboxylic acids, lactones and phenolic
14 hydroxyls, and basic groups originate from the complex aromatic system (delocalized
15 π electrons) of graphene surface. During activation, many strong oxidizing radicals
16 were produced, and eventually caused the high oxygen content of the final carbon
17 materials. For these samples, increasing activation temperature reduced the amount of
18 acidic groups and promoted the production of basic groups (see Fig. 6a and b). The
19 high temperature led to the decomposition of acidic groups into CO and CO₂, since
20 they are unstable at high temperature³⁹. Meanwhile, the high temperature promoted
21 the formation of delocalized π electrons, resulting in the high basicity¹⁸. When
22 impregnation ratio increased from 0.5 to 1.0, both acidic and basic groups increased

1 dramatically and reached a maximum at impregnation ratio of 1.5, then with
 2 impregnation ratio greater than 1.5, the amounts of these groups exhibited a slight
 3 decrease and kept high levels. As well demonstrated above that the phosphates
 4 decomposed and volatilized easily at low temperatures, during activation, less
 5 phosphoric compounds were left in the xylitol-0.2 and xylitol-0.5 samples, thus the
 6 formed oxygen groups were susceptible to the high temperature and decomposed into
 7 carbon gases. The larger impregnation ratio promoted the formation of phosphates
 8 with high degree of polymerization that tended to be stable at high temperature,
 9 whereas the large amount of phosphoric acid could hinder the thermal degradation of
 10 the oxygen groups. Accordingly, the carbon samples exhibited a slightly decrease in
 11 acidic groups with increasing impregnation ratio.

12 3.5. Evaluation of Ni(II) Adsorption Ability



13
 14 **Fig. 7. Adsorption isotherms of Ni(II) for the carbons, fitted with Langmuir isotherm model**
 15 **(dosage = 0.2 g/L, initial Ni(II) concentrations = 20-60 mg/L, initial pH = 6.0 ± 0.02,**
 16 **temperature = 25 ± 2 °C, and ionic strength = 10 mM NaCl).**

17

1 **Table 2- Ni(II) adsorption capacity of activated carbons developed from various precursor with**
 2 **phosphoric acid activation.**

Precursor	Impregnation ratio	Activation		Adsorption		S_{BET} m ² /g	Q_m mg/g	References
		Temperature °C	Time	C_0 mg/L	pH			
Xylitol	1.5	250	1 h	20-60	6.0	377	52.9	This work
Xylitol	1.5	300	1 h	20-60	6.0	432	62.9	This work
Xylitol	1.5	350	1 h	20-60	6.0	509	69.4	This work
Xylitol	1.5	350	1 h	20-60	6.0	663	64.5	This work
Phragmites australis	1.5	450	1 h	20-60	6.0	1220	35.2	This work
Lotus stalk	2	450	1 h	---	---	1220	31.0	⁴⁵
Prosopis Ruscifolia wood	2	450	0.5 h	---	---	1638	7.6	⁴⁶
Arundo donax L.	2	500	0.5 h	5-100	5.8	1194	25.8	⁴⁷
Date stone	1.75	450	2 h	10-100	---	826	24.4	⁴⁸
Wool waste	1.5	550	40 min	10-60	---	472	54.0	⁴⁹

3

4 As discussed above, phosphoric acid activation of xylitol could produce activated
 5 carbons with high surface acidity and basicity. This is very interesting considering that
 6 the produced activated carbons have application potentials in heavy metal ions
 7 removal from aqueous solution. Thus, in the present study, the adsorption properties
 8 of the xylitol-based activated carbons were evaluated by studying uptake of nickel
 9 ions from aqueous solutions. Adsorption isotherms were performed by a batch method,
 10 where 10 mg of carbon sample was added into a 150-mL conical flask with 50 mL
 11 solution of Ni(II) with an initial solution pH of 6.0. To estimate the maximum
 12 adsorption capacities of the produced activated carbons, the adsorption data were
 13 fitted with the Langmuir model ($Q_e = Q_m K_L C_e / (1 + K_L C_e)$), where Q_e and C_e are the
 14 Ni(II) equilibrium adsorption capacity (mg/g) and concentration in solution (mg/L),
 15 Q_m is the monolayer adsorption capacity of the adsorbent (mg/g), K_L is the Langmuir
 16 isotherm constant (L/mg).

17 The fitting Langmuir data for Ni(II) adsorption onto the activated carbons and a

1 reference activated carbon (AC-PA) prepared from phosphoric acid activation of
2 *Phragmites australis* (Properties: $S_{\text{BET}} = 1220 \text{ m}^2/\text{g}$, $V_{\text{tot}} = 1.098 \text{ cm}^3/\text{g}$, $V_{\text{mic}} =$
3 $0.235 \text{ cm}^3/\text{g}$, acidic groups = 1.644 mmol/g , basic groups = 1.125 mmol/g) are shown
4 in Fig. 7. The relatively high values of R^2 (> 0.98 , SI Table S1) and good
5 representation of the data (Fig. 7) indicated that the Langmuir isotherm model was
6 favorable to describe the adsorption of Ni(II) on the carbon adsorbents. The Q_{m} of the
7 carbons followed an order of AC-350-1.5 $>$ AC-450-1.5 $>$ AC-300-1.5 $>$ AC-250-1.5 $>$
8 AC-PA \gg C-250 $>$ C-300 $>$ C-350 $>$ C-450. In comparison with charcoal samples, the
9 4-7 times higher Ni(II) adsorption capacities of activated carbons was clear evidence
10 that phosphoric acid activation improved dramatically their Ni(II) adsorption
11 capacities. Compared with the reference material (AC-PA), the 170-230% larger Ni(II)
12 adsorption capacities indicated that AC-X-R could be promising adsorbents in Ni(II)
13 ions pollution cleanup. For the sake of further comparison, Table 2 also shows the
14 Ni(II) adsorption capacities of other activated carbons by phosphoric acid activation.
15 The AC-X-1.5 samples in this study showed relatively good adsorption capacities
16 compared to the adsorbents. The difference in Q_{m} of the adsorbents seems to depend
17 primarily on the surface functions, as proposed by previous papers^{26, 50, 51}. Since the
18 ionic diameter of Ni(II) is very low (0.138 nm), the surfaces of adsorbents are easily
19 accessible for Ni(II) ions, and the narrow micropore could not withdraw Ni(II)
20 effectively. Strong chemical interactions existed between the functional groups of
21 activated carbon and Ni(II) cations, such as electrostatic attraction between the
22 deprotonated acidic oxygenized groups (carboxylic, lactonic and phenolic groups) and

1 Ni²⁺ ions, ion exchange between acidic groups and Ni²⁺ ions, and complexation
2 between oxygen complexes and Ni²⁺ ions. Meanwhile, the basic groups (the
3 delocalized π electron systems of graphene layer) can form electron donor-acceptor
4 complexes with Ni²⁺ ions via the Lewis-acid-base interaction.

5 **4. CONCLUSION**

6 The results of this study demonstrated that phosphoric acid activation of xylitol
7 could produce promising carbon adsorbents with high contents of surface groups and
8 large Ni(II) adsorption capacities. The complete carbonization for phosphoric
9 acid-treated xylitol samples took place between 200 °C and 250 °C. For each
10 activation temperature, the carbon samples reached the maximum surface area, and
11 content of surface groups at impregnation ratio of 1.5. Compared with the charcoal
12 obtained from pyrolysis of xylitol, the activated carbon showed much larger yields,
13 surface area, surface groups content, and Ni(II) adsorption capacity.

14 **ASSOCIATED CONTENT**

15 **Supporting Information Available**

16 Table S1 summarizes the Langmuir model fitting parameters of the nickel adsorption
17 onto the carbons. Figure S1 presents Raman spectra and intensity ratios of D to G
18 bands of the activated carbons. Figure S2 presents SEM micrographs of C-X and AC
19 samples.

20 **ACKNOWLEDGEMENTS**

21 This work was supported by the Independent Innovation Foundation of Shandong
22 University (2012JC029), Natural Science Foundation for Distinguished Young

1 Scholars of Shandong Province (JQ201216) and National Water Special Project
2 (2012ZX07203-004). The authors gratefully acknowledge the fund from Shanghai
3 Tongji Gao Tingyao Environmental Science and Technology Development
4 Foundation.

5 REFERENCES

- 6 1. A. Bhatnagar, W. Hogland, M. Marques and M. Sillanpää, *Chem. Eng. J.*,
7 2013, **219**, 499-511.
- 8 2. J. E. Kilduff, T. Karanfil and W. J. Weber, *Environ. Sci. Technol.*, 1996, **30**,
9 1344-1351.
- 10 3. G. Yang, L. Tang, Y. Cai, G. Zeng, P. Guo, G. Chen, Y. Zhou, J. Tang, J. Chen
11 and W. Xiong, *RSC Adv.*, 2014, **4**, 58362-58371.
- 12 4. M. Molina-Sabio, M. T. Gonzalez, F. Rodriguez-Reinoso and A.
13 Sepúlveda-Escribano, *Carbon*, 1996, **34**, 505-509.
- 14 5. M. Oschatz, L. Borchardt, I. Senkovska, N. Klein, M. Leistner and S. Kaskel,
15 *Carbon*, 2013, **56**, 139-145.
- 16 6. Z. Huang, H. Shao, B. Huang, C. Li, Y. Huang and X. Chen, *RSC Adv.*, 2014,
17 **4**, 18737-18743.
- 18 7. M. Myglovets, O. I. Poddubnaya, O. Sevastyanova, M. E. Lindström, B.
19 Gawdzik, M. Sobiesiak, M. M. Tsyba, V. I. Sapsay, D. O. Klymchuk and A. M.
20 Puziy, *Carbon*, 2014, **80**, 771-783.
- 21 8. P.-T. Yeung, P.-Y. Chung, H.-C. Tsang, J. Cheuk-On Tang, G. Yin-Ming Cheng,
22 R. Gambari, C.-H. Chui and K.-H. Lam, *RSC Adv.*, 2014, **4**, 38839-38847.

- 1 9. L. Nielsen, M. J. Biggs, W. Skinner and T. J. Bandoz, *Carbon*, 2014, **80**,
2 419-432.
- 3 10. D. Ding, Y. Zhao, S. Yang, W. Shi, Z. Zhang, Z. Lei and Y. Yang, *Water Res.*,
4 2013, **47**, 2563-2571.
- 5 11. V. J. Watson, C. Nieto Delgado and B. E. Logan, *Environ. Sci. Technol.*, 2013,
6 **47**, 6704-6710.
- 7 12. L. K. C. de Souza, N. P. Wickramaratne, A. S. Ello, M. J. F. Costa, C. E. F. da
8 Costa and M. Jaroniec, *Carbon*, 2013, **65**, 334-340.
- 9 13. P. Chingombe, B. Saha and R. J. Wakeman, *Carbon*, 2005, **43**, 3132-3143.
- 10 14. B. Beckingham and U. Ghosh, *Environ. Sci. Technol.*, 2011, **45**, 10567-10574.
- 11 15. H. Liu, W. Liu, J. Zhang, C. Zhang, L. Ren and Y. Li, *J. Hazard. Mater.*, 2011,
12 **185**, 1528-1535.
- 13 16. H. Liu, J. Zhang, N. Bao, C. Cheng, L. Ren and C. Zhang, *J. Hazard. Mater.*,
14 2012, **235–236**, 367-375.
- 15 17. S. Zuo, J. Liu, J. Yang and X. Cai, *Carbon*, 2009, **47**, 3578-3580.
- 16 18. D. Prahas, Y. Kartika, N. Indraswati and S. Ismadji, *Chem. Eng. J.*, 2008, **140**,
17 32-42.
- 18 19. A. J. Romero-Anaya, M. A. Lillo-Ródenas, C. Salinas-Martínez de Lecea and
19 A. Linares-Solano, *Carbon*, 2012, **50**, 3158-3169.
- 20 20. A. M. Puziy, O. I. Poddubnaya, R. P. Socha, J. Gurgul and M. Wisniewski,
21 *Carbon*, 2008, **46**, 2113-2123.
- 22 21. E.-A. Kim, A. L. Seyfferth, S. Fendorf and R. G. Luthy, *Water Res.*, 2011, **45**,

- 1 453-460.
- 2 22. M. I. Bautista-Toledo, J. Rivera-Utrilla, R. Ocampo-Pérez, F. Carrasco-Marín
3 and M. Sánchez-Polo, *Carbon*, 2014, **73**, 338-350.
- 4 23. Y. Ono, Y. Amano, T. Nakamura and M. Machida, *Carbon*, 2012, **50**, 4984.
- 5 24. X. Tian, G. Hong, Y. Liu, B. Jiang and Y. Yang, *RSC Adv.*, 2014, **4**,
6 36316-36324.
- 7 25. B. Hong, X. Yu, L. Jiang, H. Xue, F. Liu, J. Li and Y. Liu, *RSC Adv.*, 2014, **4**,
8 33574-33577.
- 9 26. H. Liu, P. Dai, J. Zhang, C. Zhang, N. Bao, C. Cheng and L. Ren, *Chem. Eng.*
10 *J.*, 2013, **228**, 425-434.
- 11 27. H. Liu, J. Zhang, C. Zhang, N. Bao and C. Cheng, *Carbon*, 2013, **60**, 289-291.
- 12 28. J. Wang, H. Liu, S. Yang, J. Zhang, C. Zhang and H. Wu, *Appl. Surf. Sci.*,
13 2014, **316**, 443-450.
- 14 29. Y. Kuno, M. Kojima, S. Ando and H. Nakagami, *J. Control. Release*, 2005,
15 **105**, 16-22.
- 16 30. J. J. M. Órfão, A. I. M. Silva, J. C. V. Pereira, S. A. Barata, I. M. Fonseca, P. C.
17 C. Faria and M. F. R. Pereira, *J. Colloid Interf. Sci.*, 2006, **296**, 480-489.
- 18 31. F. Suárez-García, A. Martínez-Alonso and J. M. D. Tascón, *Carbon*, 2004, **42**,
19 1419-1426.
- 20 32. M. A. Nahil and P. T. Williams, *Biomass Bioenergy*, 2012, **37**, 142-149.
- 21 33. H. Teng, T.-S. Yeh and L.-Y. Hsu, *Carbon*, 1998, **36**, 1387-1395.
- 22 34. Z.-L. Xie, R. J. White, J. Weber, A. Taubert and M. M. Titirici, *J. Mater.*

- 1 *Chem.*, 2011, **21**, 7434-7442.
- 2 35. V. Fierro, V. Torné-Fernández and A. Celzard, *Micropor. Mesopor. Mat.*, 2006,
3 **92**, 243-250.
- 4 36. N. M. Haimour and S. Emeish, *Waste Manage.*, 2006, **26**, 651-660.
- 5 37. C. Srinivasakannan and M. Zailani Abu Bakar, *Biomass Bioenergy*, 2004, **27**,
6 89-96.
- 7 38. L. Wang, Y. Guo, B. Zou, C. Rong, X. Ma, Y. Qu, Y. Li and Z. Wang,
8 *Bioresource Technol.*, 2011, **102**, 1947-1950.
- 9 39. Y. Guo and D. A. Rockstraw, *Carbon*, 2006, **44**, 1464-1475.
- 10 40. V. Gómez-Serrano, E. M. Cuerda-Correa, M. C. Fernández-González, M. F.
11 Alexandre-Franco and A. Macías-García, *Mater. Lett.*, 2005, **59**, 846-853.
- 12 41. V. Fierro, G. Muñoz, A. H. Basta, H. El-Saied and A. Celzard, *J. Hazard.*
13 *Mater.*, 2010, **181**, 27-34.
- 14 42. Y. Guo and D. A. Rockstraw, *Micropor. Mesopor. Mater.*, 2007, **100**, 12-19.
- 15 43. A. M. Puziy, O. I. Poddubnaya, A. Martínez-Alonso, F. Suárez-García and J.
16 M. D. Tascón, *Carbon*, 2002, **40**, 1493-1505.
- 17 44. A. M. Puziy, O. I. Poddubnaya, A. Martínez-Alonso, F. Suárez-García and J.
18 M. D. Tascón, *Carbon*, 2005, **43**, 2857-2868.
- 19 45. L. Huang, Y. Sun, T. Yang and L. Li, *Desalination*, 2011, **268**, 12-19.
- 20 46. D. Nabarlantz, J. de Celis, P. Bonelli and A. L. Cukierman, *J. Environ. Manage.*,
21 2012, **97**, 109-115.
- 22 47. M. C. Basso, E. G. Cerrella and A. L. Cukierman, *Ind. Eng. Chem. Res.*, 2002,

1 **41**, 3580-3585.

2 48. F. Bouhamed, Z. Elouear, J. Bouzid and B. Ouddane, *Fresen. Environ. Bull.*,
3 2013, **22**, 3490-3500.

4 49. Q. Gao, H. Liu, C. Cheng, K. Li, J. Zhang, C. Zhang and Y. Li, *Powder*
5 *Technol.*, 2013, **249**, 234-240.

6 50. H. Liu, X. Wang, G. Zhai, J. Zhang, C. Zhang, N. Bao and C. Cheng, *Chem.*
7 *Eng. J.*, 2012, **209**, 155-162.

8 51. H. Liu, S. Liang, J. Gao, H. H. Ngo, W. Guo, Z. Guo, J. Wang and Y. Li, *Chem.*
9 *Eng. J.*, 2014, **246**, 168-174.

10

11

12

13

14

15

16

17

18

19

20

21

22 **FIGURE CAPTIONS:**

- 1 **Fig. 1.** TGA (a) and DTG (b) curves for pyrolysis of xylitol and xylitol-R samples.
- 2 **Fig. 2.** XRD patterns of charcoals (a) derived from pyrolysis of xylitol and AC-X-R
- 3 samples produced at activation temperatures of 150 (b), 200 (c), and 250 °C (d).
- 4 **Fig. 3.** Yields of the produced carbon materials (Yield is defined as the % ratio of
- 5 weight of carbon produced to the weight of xylitol utilized for activation/pyrolysis).
- 6 **Fig. 4.** BET surface area calculated by the standard BET method of the carbon
- 7 materials.
- 8 **Fig. 5.** N₂ adsorption/desorption isotherms (a) and DFT pore size distributions (b) for
- 9 carbons prepared with impregnation ratio of 1.5 at different activation temperatures.
- 10 **Fig. 6.** XPS survey spectra of C-X and AC-X-1.5 samples (a). The Boehm's titration
- 11 results of the carbons: acidity (b), basicity (c), and total groups (d).
- 12 **Fig. 7.** Adsorption isotherms of Ni(II) for the carbons, fitted with Langmuir isotherm
- 13 model.